Journal of Structural Geology, Vol. 7, Nos. 3/4, pp. 281 to 300, 1985
Printed in Great Britain

0191-8141/85 $03.00 + 0.00

Megakinking in the Lachlan Fold Belt, Australia

C. McA. Powell, J. P. Cole and T. J. Cudahy

Australian Plate Research Group, School of Earth Sciences, Macquarie University, North Ryde, N.S.W. 2113, Australia
with an Appendix by N. I. Fisher, CSIRO Division of Mathematics and Statistics, P.O. Box 218, Lindfield, N.S.W. 2070, Australia

(*Received* 8 *February* 1984; *accepted in revised form* 2 *August* 1984)

Abstract—The regional N–S tectonic grain of the easternmost Lachlan Fold Belt is produced by upright tight folds with well-developed quasi-vertical axial-surface foliation, and comprises domains in which the early folds and foliation have consistent orientation. The domains are up to a few tens of kilometres along trend, and are separated by narrow zones across which the tectonic grain swings, commonly by 20 to 30°, to produce a regional tectonic kink pattern. These megakinks have both sinistral (070 ± 10°) and dextral (110 ± 10°) trends—the dextral zones being more common. In the megakink bands, which may be up to 10 km wide, there are commonly second-order kink zones, a few hundred metres wide, in which the pre-existing fold trends are rotated 90°, or more, from their regional N–S trend. Small-scale kink bands of metre to millimetre width are much more common in the megakink bands than in the planar domains between. Outcrop-scale kink folds were formed by a subhorizontal principal compression acting parallel to the tectonic grain, even where that grain is more than 90° oblique to the regional trend. Outcrop-scale kinks are thus interpreted to have formed first under regional N–S compression, with the megakink domains rotating later. The megakinking event is mid-Carboniferous (*c.* 330 Ma), being younger than the regional Early Carboniferous folding and older than the latest Carboniferous basal sediment of the Sydney Basin. The megakinks appear to have nucleated along strike of pre-existing ESE- and ENE-trending lineaments in the Lachlan Fold Belt, possibly under continent-wide N–S compression.

INTRODUCTION

Kink bands and associated structures are widely recognized as minor, commonly late, structures in the evolution of fold belts (e.g. Anderson 1968, Clifford 1968, Dewey 1965, 1966, Fyson 1966, Hobson 1973, Marshall 1964, Ramsay 1962). Kink structures develop in foliated terranes where earlier deformation has imparted a strong mechanical anisotropy to the rocks. Generally, kinks are small structures, centimetres to metres wide, although Weiss (1968) pointed out that larger kink bands are possible in thickly layered terranes. The largest documented kink bands have widths of hundreds of metres, and occur in weakly deformed rocks where beds, or packets of beds, provide the mechanical anisotropy (e.g. Collomb & Donzeau 1974, Rixon *et al.* 1983).

In the southeastern part of the mid-Palaeozoic Lachlan Fold Belt of Eastern Australia (Fig. 1), the Ordovician turbidite succession has been deformed into a series of tight, upright folds with a well-developed differentiated crenulation cleavage, S_1, parallel to the fold axial surface (Williams 1971, 1972, Cole 1982, Wilson *et al.* 1982, Powell 1983a). The earliest recognizable mesoscopic folds, F_1, have subhorizontal axes with gentle plunges to the north and south. A second phase of deformation has rotated the F_1 folds to a recumbent orientation in narrow domains (e.g. at Bermagui, Williams 1971, Powell 1983a), but for most of the N.S.W. south coast region, the F_1 structures are upright, and are the only significant structures influencing the nature and orientation of the bedding and foliation.

In the coastal strip, and for up to 30 km inland (Fig. 2), S_1 has a stripy appearance with alternating quartzose and micaceous bands in the hinges and limbs, respectively, of microfolds associated with the differentiated crenulation cleavage (see Williams 1982). The degree of 'stripiness' increases inland, where it is difficult to recognize bedding in many outcrops because of the S_1 overprint. The stripy cleavage zone abuts sharply against an inland zone of slaty cleavage, approximately along the line of the Budawang Synclinorium (Fig. 2). The abrupt change in cleavage and deformation style across the Budawang Synclinorium may correspond to the boundary between the Middle and Late Ordovician fore-arc basin terrane to the west and subduction complex to the east (Powell 1983a,b).

During mapping of the coastal terrane at 1:25,000, we found that there were large domains, commonly 10 km or more long in the direction of the N–S tectonic grain, where all the F_1 structural elements (π_1^0, S_1 and L_1^0) (see Fig. 10) are consistent in orientation. At the boundaries of the domains, the attitude of the structural elements changes orientation sharply, over distances of tens to hundreds of metres, by angles commonly around 20 to 30°. When viewed at regional map scale, these sharp angular changes in F_1 orientation appear as kinks in the regional structure, and this led Powell (1983a, 1984) to postulate megakinks in the tectonic grain of the Lachlan Fold Belt. In this paper we describe first the geometry of the Bermagui megakink band, and then other possible megakinks in the easternmost Lachlan Fold Belt.

THE BERMAGUI MEGAKINK BAND

Background

The Bermagui megakink band (Fig. 3) was selected for detailed study because it was where megakinking of the Lachlan Fold Belt was first recognized (Powell

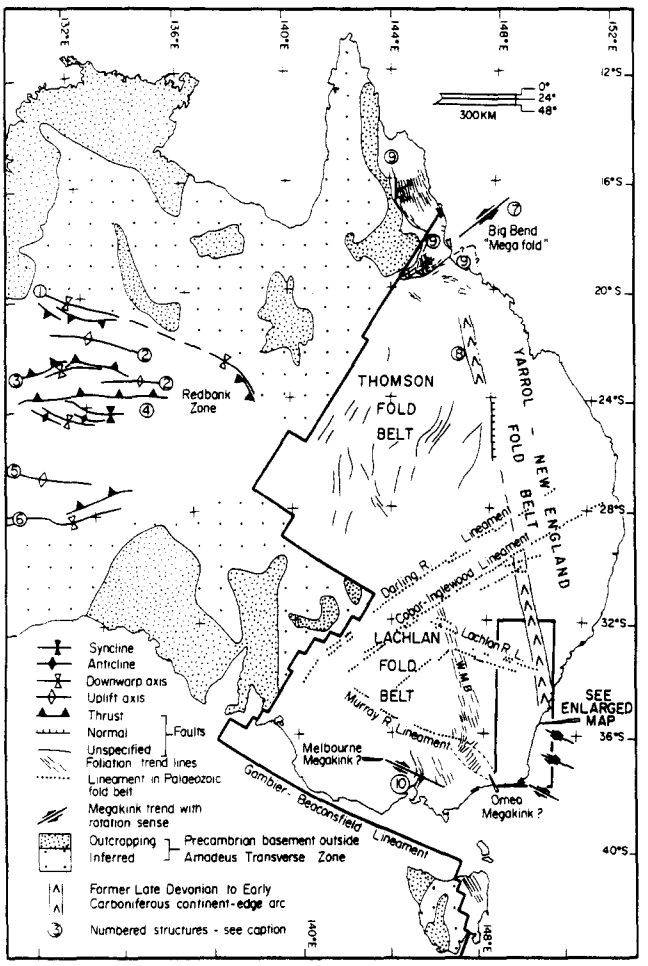

Fig. 1. Mid-Carboniferous structural sketch map of the eastern two-thirds of Australia based on the Tectonic Map of Australia (Geological Society of Australia 1971). Heavy line marking the edge of the proven Precambrian basement is the Tasman Line. The Yarrol–New England Fold Belt was a continental slope-to-trench terrane at the time. Numbered structures: 1, Lander Trough and Toko Syncline; 2, Arunta Block; 3, Thrust-faulted northern edge of the Ngalia Basin; 4, Amadeus Basin; 5, Musgrave Block; 6, Officer Basin; 7, Big Bend Megafold; 8, Anakie Inlier; 9, Palmerville–Burdekin–Clarke River Fault; 10, Steiglitz area. WMB, Wagga Metamorphic Belt. Modified from Powell (1984, fig. 4).

1983a) and the inland outcrop is generally good. The megakink band is located east of the intersection of the NE-trending Tantawangalo Fault (a wrench fault with 16 km of mid-Devonian dextral movement) and the N-trending boundary between the foliated stripy coastal, and the massive to slaty inland, Ordovician facies (Fig. 2). There is a great mechanical contrast in rock types across the Tantawangalo Fault, and also across the stripy-slaty cleavage contact, with massive Lower to Middle Devonian granitoids of the Bega Batholith to the west and fissile foliated Ordovician turbidites to the east.

Cudahy (1983) extended the regional reconnaissance mapping reported in Powell (1983a), and re-examined each outcrop to determine the nature and orientation of a variety of outcrop-scale structures. The revised map (Fig. 3) shows the structure to be more complex than initially envisaged (Powell 1983a, fig. 27a), with a number of domains of relatively constant F_1 orientation between the N and NNE trend further north and south. In addition, there is a narrow zone of highly rotated F_1 structural elements (the Murrah kink zone, Fig. 2)

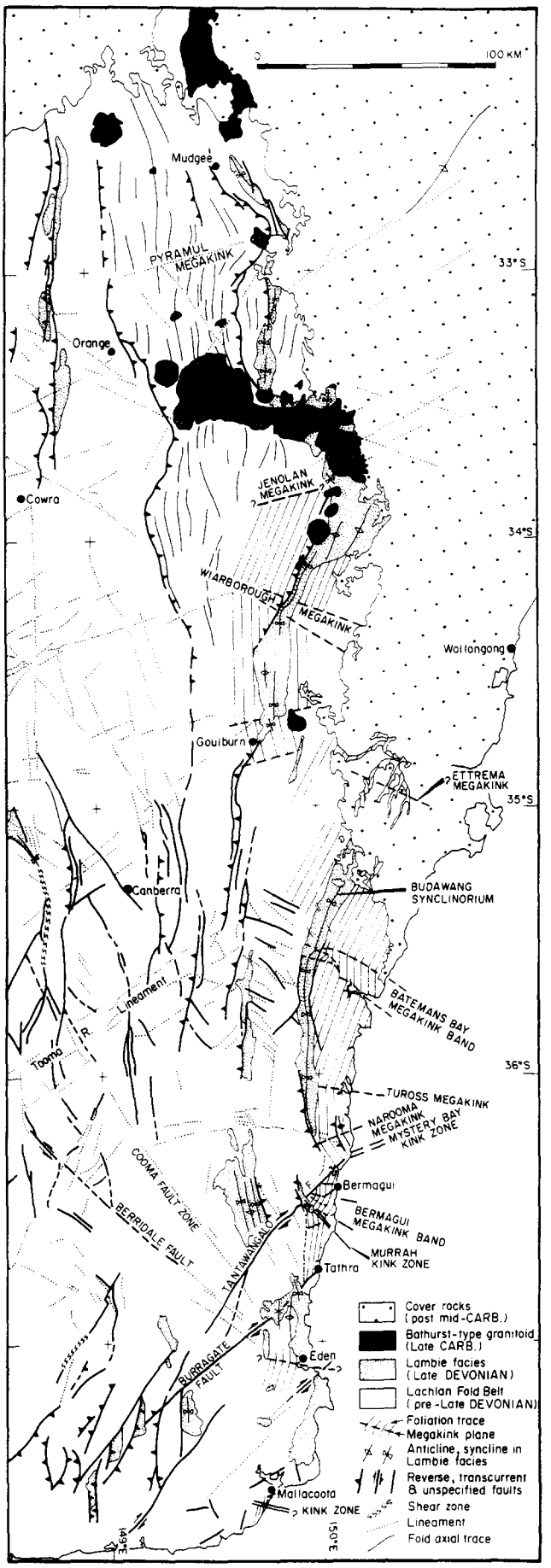

Fig. 2. Structural map of the eastern Lachlan Fold Belt. Adapted from Scheibner (1974a) with updates from the structural map of New South Wales (Scheibner in prep.) and the geometry of the megakinked terrane from this work. A more detailed map of the coastal strip between 35°15′S and 36°55′S appears in Powell (1984, fig. 1).

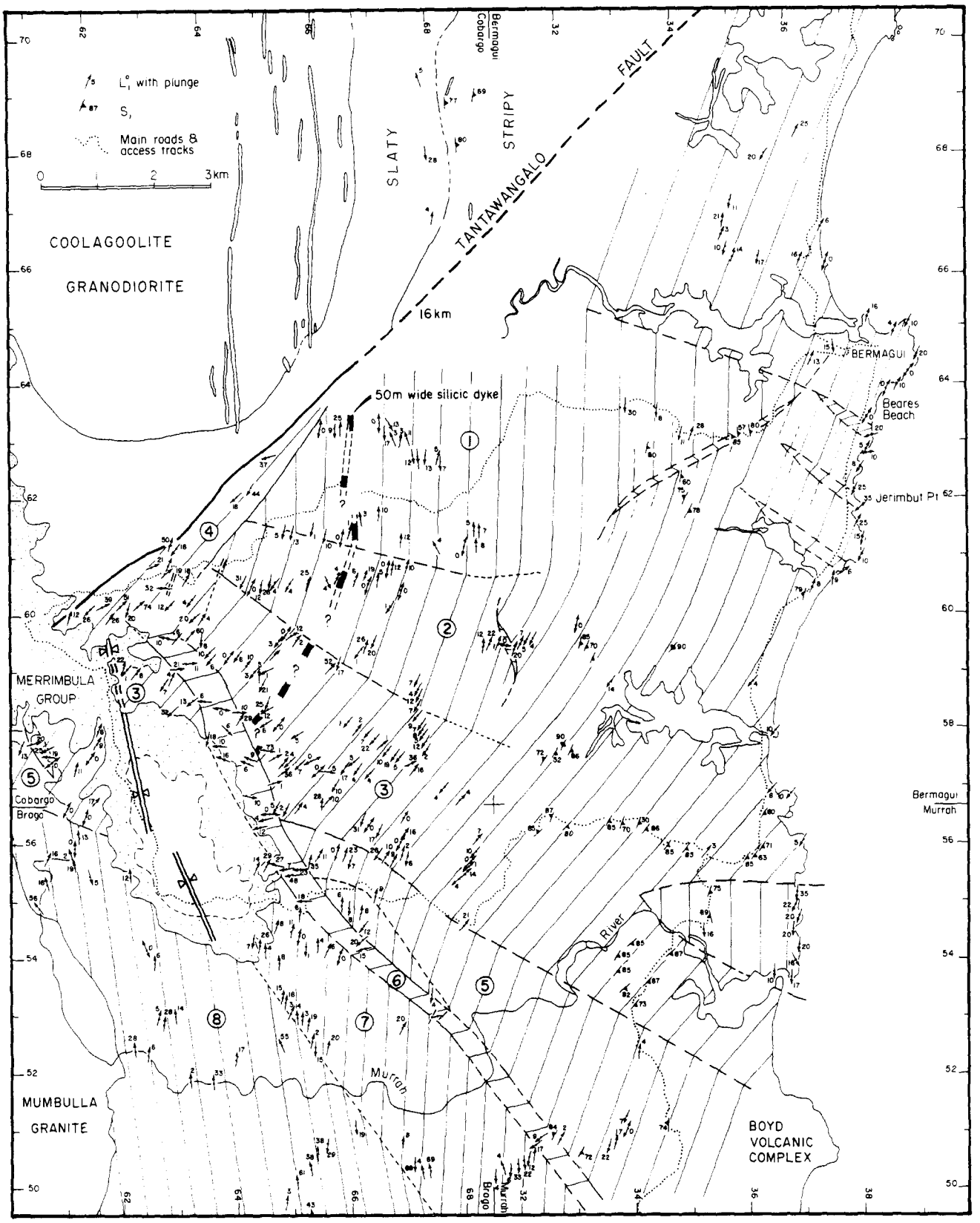

Fig. 3. F_1 axial trends in the Bermagui megakink. Short arrows represent individual outcrop trends calculated mainly from bedding and cleavage intersections. Barbed lines are S_1 cleavage measurements. Thin continuous lines represent the best-fit megakink interpretation with full, dashed and dotted lines marking definite, probable and possible domain boundaries, respectively. Data presented are only a portion of those measured in some places. The map was drawn initially at 1:25,000 from the Cobargo, Brogo, Bermagui and Murrah topographic maps.

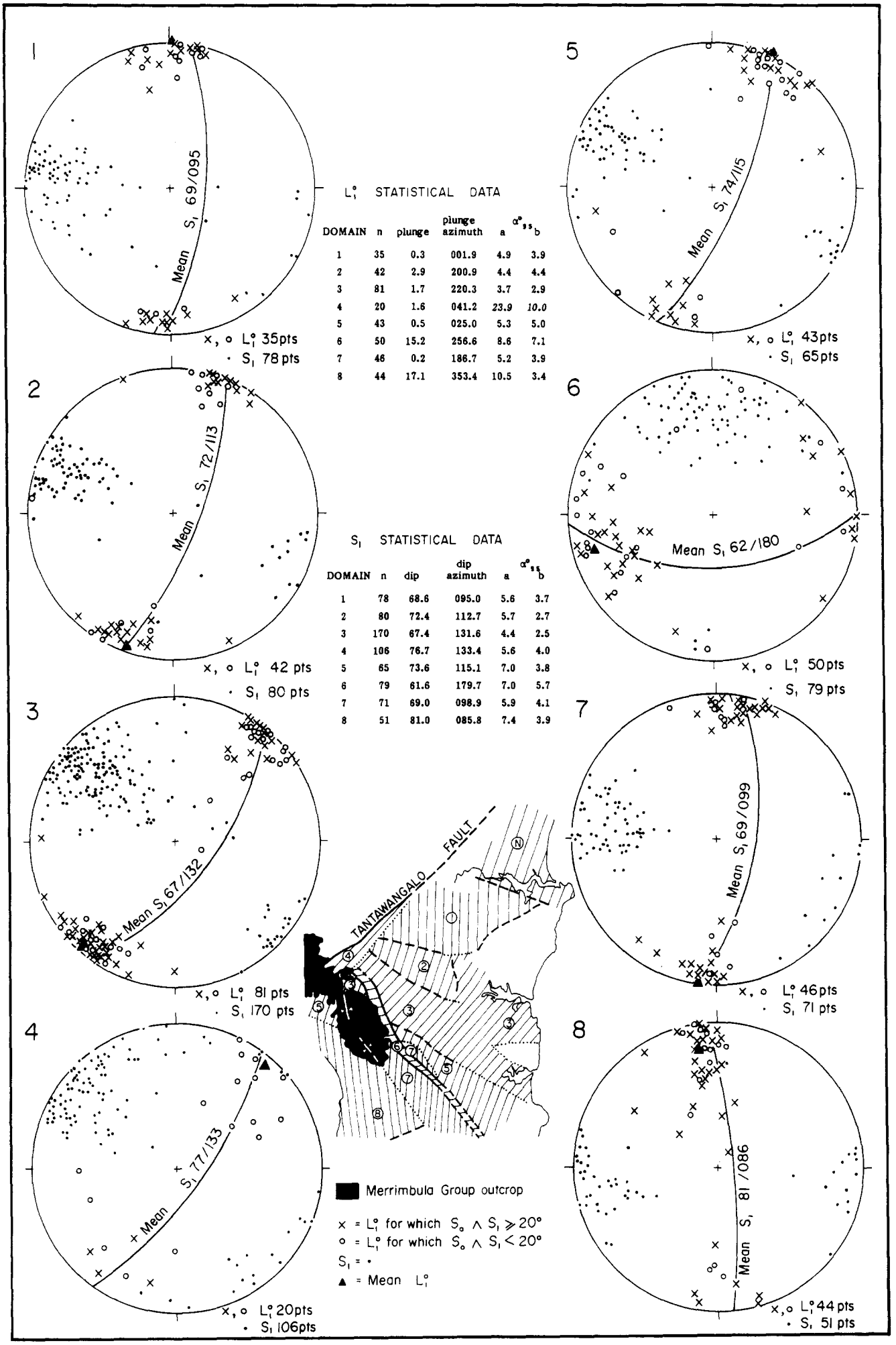

L1° STATISTICAL DATA

DOMAIN	n	plunge	plunge azimuth	a	α°_{95} b
1	35	0.3	001.9	4.9	3.9
2	42	2.9	200.9	4.4	4.4
3	81	1.7	220.3	3.7	2.9
4	20	1.6	041.2	23.9	10.0
5	43	0.5	025.0	5.3	5.0
6	50	15.2	256.6	8.6	7.1
7	46	0.2	186.7	5.2	3.9
8	44	17.1	353.4	10.5	3.4

S1 STATISTICAL DATA

DOMAIN	n	dip	dip azimuth	a	α°_{95} b
1	78	68.6	095.0	5.6	3.7
2	80	72.4	112.7	5.7	2.7
3	170	67.4	131.6	4.4	2.5
4	106	76.7	133.4	5.6	4.0
5	65	73.6	115.1	7.0	3.8
6	79	61.6	179.7	7.0	5.7
7	71	69.0	098.9	5.9	4.1
8	51	81.0	085.8	7.4	3.9

extending southeasterly across the ESE-trending megakink band along the eastern margin of the outcrop of Upper Devonian sediments.

Analytical procedure

The Bermagui megakink band has been mapped at 1:25,000 with more detailed mapping on the coast, and in the relatively well-exposed western part. The resultant map shows measured L_1^0 or small-scale π_1^0 axes, with S_1 data plotted only where scarce outcrop did not permit measurement of sufficient L_1^0 axes. Because of the scale of the map, only representative data are shown in the areas of best exposure, but all data have been used in stereograms (Fig. 4). The positions of domain boundaries have been selected by eye, using an underlay of parallel ruled lines to pick first the best estimate of F_1 trend within a potential domain, and then the position at which the F_1 orientation changes to the next domain. Although there is subjectivity in selecting domains by this procedure, the statistical parameters calculated from the data in each domain (see below) show that the domains selected are significantly different in orientation from their neighbours at the 95% confidence level. The confidence we attach to each domain boundary is indicated in the caption to Fig. 3 by a three-fold categorization.

Orientation data from each domain were first plotted on stereographic projection, and then analysed statistically using programs of N. I. Fisher (described in Appendix). The results (statistics plotted on Fig. 4) show that the mean S_1 for each domain can be determined to within 4 to 7° at the 95% confidence level, and that mean L_1^0 is determined to within 5° in five of the eight domains. Domain 4, with the least well-constrained mean L_1^0, is an elongate domain adjacent to the Tantawangalo Fault, and may have a more complex structure than can be represented in Fig. 3. Domain 6 is the Murrah kink zone and can be shown (Fig. 5) to be internally folded, especially adjacent to the Upper Devonian Merrimbula Group. The large confidence interval in domain 8 reflects a number of moderately steep L_1^0 axes in this area lying adjacent to the Mumbulla Granite, and may represent some contact strain during its mid-Devonian intrusion.

Geometry of domains within the megakink band

The Bermagui megakink band represents a dextral bend in the regional foliation with an amplitude of 2–3 km (Cudahy 1983). Within this bend, eight domains have been defined (Figs. 3 and 4). The angular change from one domain to the next has been estimated using the mean S_1 and L_1^0 values for each domain, and these estimates are tabulated in Fig. 6(d). For most of the domains, the angular change is between 15 and 35° (mean of six angular changes is 21°, standard deviation 7.4°). Higher interdomain angles around 60° occur where the Murrah kink zone (domain 6) adjoins domains 5 and 7, and an intermediate value of 44° occurs between domains 3 and 6.

The Murrah kink zone is the domain most highly rotated from the regional N–S grain. This zone is more complexly deformed than can be shown in Fig. 3, and appears to cut across domains 3, 5 and 7. In the map (Fig. 3), the megakink interpretation has been extended to include structures on the coast, where outcrop provides good control. However, the segmented pattern recognized in the western half of the megakink band may not continue to the coast, just as the N-trending domain on the coast north of the Murrah River does not appear to continue far inland.

Summary stereograms

The summary stereograms (Figs. 6a & b) show the great scatter of S_1 poles and L_1^0 intersections derived by plotting data from the entire megakink band, and contrast with the well-defined orientations in the map-linear domains (Figs. 3 and 4). The synoptic diagram of mean direction of S_1 and L_1^0 from each domain (Fig. 6c) shows that the mean S_1 poles lie along a great circle about an axis plunging 67° towards 150°, which is inferred to be the megakink rotation axis for the western half of the map area. The distribution of the mean L_1^0 axes is approximately along a 79°-small circle about the rotation axis.

These orientations are consistent with S_1 of an initial mean orientation dipping 73° towards 105°, and L_1^0 pitching 5° to the north, having been rotated about an axis pitching 74° to the south in the mean S_1. The assumed initial S_1 orientation lies between the mean S_1 orientation of 62°/105° in the area immediately to the north, and 79°/102° in the area just to the south, of the Bermagui megakink band—both areas having subhorizontal π_1^0 axes. The 79°-small circle for the rotation of L_1^0 axes accounts for the horizontal to gentle northerly plunges of L_1^0 in the more northerly trending domains (1, 7 and 8 of Fig. 4) and the increasingly southward plunges in domains rotated most from the assumed 015°-trending initial orientation (domains 3 and 6 of Fig. 4).

Fig. 4. F_1 structural data on equal-area lower-hemisphere stereograms for eight domains of the Bermagui megakink band. Data mainly from Cudahy (1983). Statistics computed by N. I. Fisher (see Appendix). 95% confidence cones in italics are less reliable than those in upright numerals, because $n < 25$. **a** and **b** are the angular magnitudes of the major and minor semi-axes of the 95% elliptical confidence cone. Independent checks using programs written by P. Fell and J. Cole from the equations in Cheeney (1983) gave identical results for the mean π_1^0, L_1^0 and S_1 attitudes, and similar 95% confidence cones—the minor differences being attributable to the difference in mathematical procedure between Fisher's method and the Bingham technique described in Cheeney (1983). In each case, the confidence cone calculated by the Bingham technique is slightly tighter than the major axis calculated by Fisher's technique, and we have taken the conservative approach of using the looser cone of confidence in reporting our data.

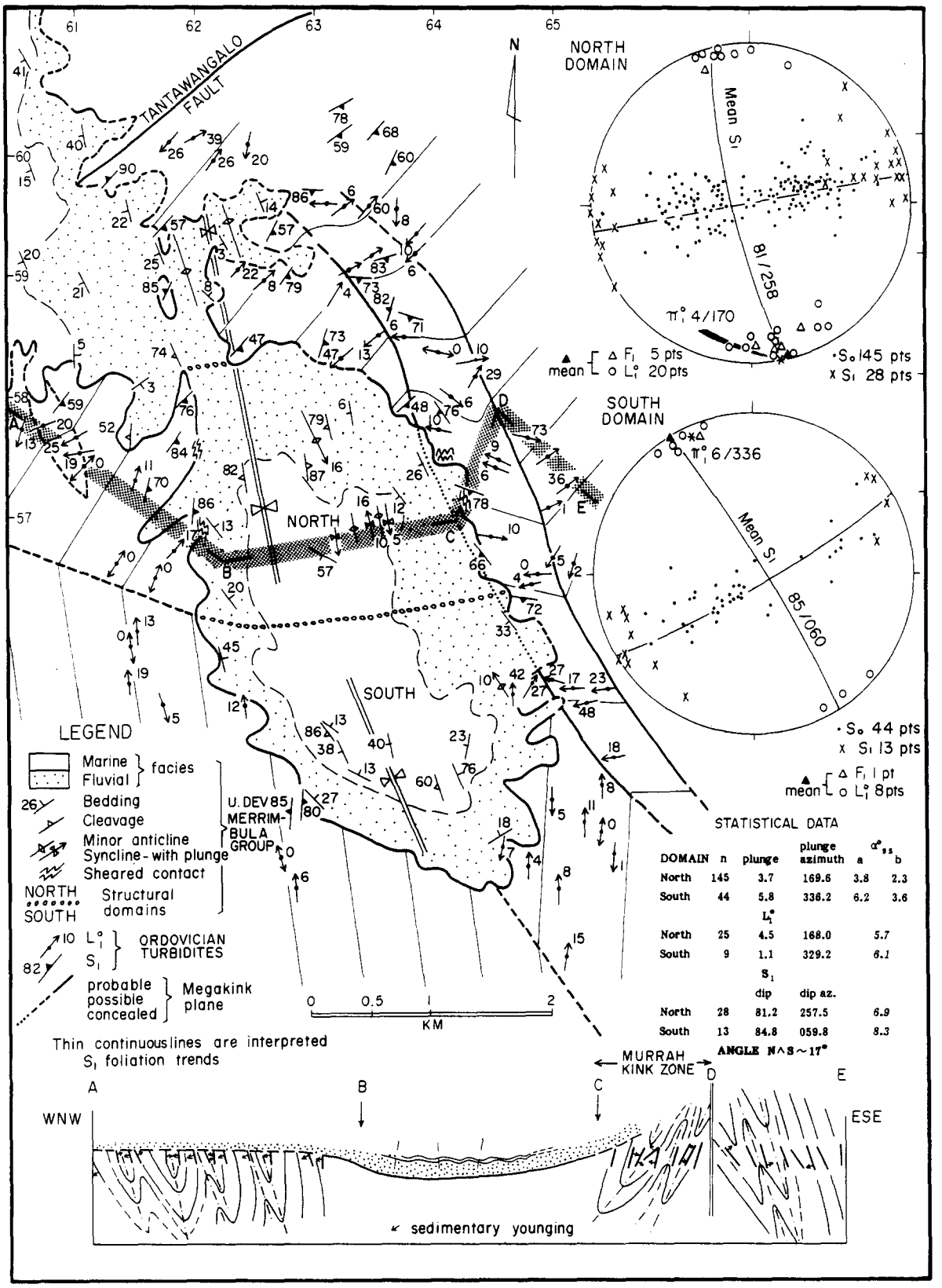

Fig. 5. Structural map of the Upper Devonian Merrimbula Group and subjacent deformed Ordovician turbidites. Only representative structural measurements are shown, with all data from two domains in the Merrimbula Group shown in the stereograms. For continuation to northwest see Powell (1983a, fig. 26). Cobargo and Brogo 1:25,000 Grid reference ticks shown. Composite cross-section is along lines A–E, normal to local tectonic trends.

Second-order kink zones

Within the Bermagui megakink band, there are several smaller kink zones where the foliation is rotated well out of the regional trend. The most prominent of these is the Murrah kink zone (Fig. 5), which varies in width from 200 m up to almost 1 km. Other second-order kink zones occur on the coast just south of Bermagui, at Beares Beach and Jerimbut Point (Fig. 3). The density of outcrop-scale kink bands, buckle folds and kink-

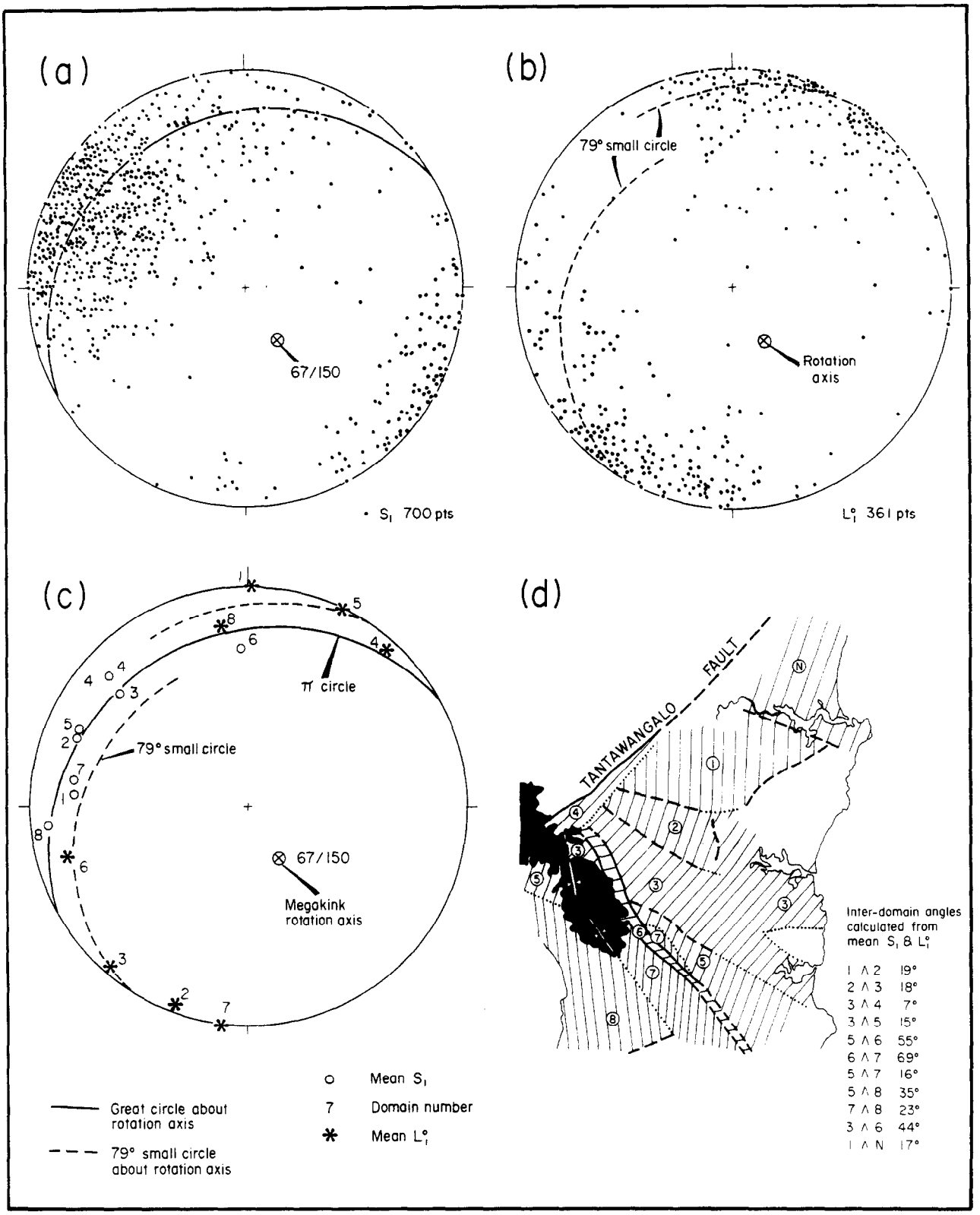

Fig. 6. Summary equal-area lower-hemisphere stereograms for the Bermagui megakink band. (a) S_1. (b) L_1^0. (c) Relationship of mean directions of S_1 and L_1^0 in each domain to the inferred rotation axis. (d) Calculated angles between adjacent subdomains.

related crenulation cleavage is much higher in these second-order kink zones than elsewhere, and the geometry of the foliation within the second-order kink zones is far from constant—in contrast to the various other domains of the megakink band. The Beares Beach and Jerimbut Point kink zones appear to contain relatively planar domains a few tens of metres in length along strike, showing a relationship to the second-order kink zones analogous to the relationship of the larger domains to the Bermagui megakink band. The Murrah kink zone contains large sinusoidal to chevron-style folds, of tens of metres wavelength.

In places where outcrop is good (such as at Beares Beach and Jerimbut Point) second-order kink-zone

boundaries are seen to be marked by a progressive change in orientation over a few metres or tens of metres. In other places (e.g. near GR 314592 Bermagui and GR 353629 Bermagui), the probable presence of a second-order kink zone 100 m or more wide is indicated only by an abrupt change in orientation from one outcrop to the next. A second-order kink zone in domain 5 just west of the Merrimbula Group syncline (GR 610575 Cobargo, Figs. 3 and 5) appears to be a lens within the megakink subdomain.

Relation of outcrop-scale kinks to the megakink

Outcrop-scale kinks of both dextral and sinistral symmetry occur in all domains of the Bermagui megakink band, and are most common around the Upper Devonian synclinal keel. Figures 7 and 8 show examples from the Mystery Bay kink zone, at the southern boundary of the sinistral Narooma megakink band (Fig. 2). Although these are not within the Bermagui megakink band, the geometry illustrated is typical of minor kink folds wherever they occur in the N.S.W. south coast region. The kink bands invariably have steeply plunging kink axes, and symmetry consistent with horizontal shortening along the direction of the local S_1, with extension normal to it.

Figure 9 details the proportions of dextral and sinistral minor kinks from within the Bermagui megakink band. The proportion of sinistral to dextral kink bands in each domain can be interpreted in the light of experiments by Gay & Weiss (1974) who investigated the effect of the maximum principal compression, σ_1, lying oblique by an angle, α, to the foliation being kinked. Gay & Weiss (1974) showed that for $\alpha \leq 5°$ both sets of kink bands were developed; where $5° \leq \alpha \leq 15°$ one set of kinks was dominant, and for $15° \leq \alpha \leq 30°$ deformation was accomplished by a combination of kinking in one direction and sliding along the foliation in the other direction. Treating those domains with roughly equal proportions of sinistral and dextral kink bands as having $\alpha \leq 5°$, and those with one direction dominant over the other as having $5° \leq \alpha \leq 30°$, the present orientation of the maximum principal stress, σ_1, in each of the domains of the Bermagui megakink band can be estimated (Fig. 9a). There is a swing of a little more than 90° in σ_1 from N–S in domain 1 to E–W in the second-order Murrah kink zone, and a complementary swing back to N–S south of the Bermagui megakink band. In the western third of the area (domains 3, 4, 5 and 8 in Fig. 9a), σ_1 is consistently oriented counterclockwise from the S_1 foliation, whereas in two of the domains just east of the Merrimbula Group syncline (3 and 6 in Fig. 9a), σ_1 is oriented clockwise from the S_1 foliation.

A completely independent method of calculating the orientation of σ_1 by bisecting the appropriate angle between the conjugate kink planes (Ramsay 1962, Dewey 1965) gives σ_1 orientations lying within 5° of S_1 in all domains, though commonly the inferred σ_1 direction lies on the opposite side of S_1 from that inferred by the kink-proportion method. We are currently evaluating the significance of the difference between these two methods, but our principal conclusions here, namely that σ_1 was essentially subhorizontal and parallel to S_1, stands independent of the method used in its calculation.

The pattern of stress trajectories that would have existed if the outcrop-scale kinks were formed with the regional S_1 foliation in its present postion (Fig. 9a), would have been complex. A simpler pattern is obtained if the regional foliation is rotated to a common direction, assumed to be N–S in Fig. 9(b). Two general conclusions can be drawn from these data. First, because of the simple regional stress pattern implied, we think it likely that the outcrop-scale kink bands formed early in the megakinking deformation when the regional foliation had a constant orientation. Secondly, there are differences in both the density of kink bands and the proportion of sinistral to dextral kinks, which can be related to position relative to the Merrimbula Group outcrop, thereby suggesting that either a pre-existing, or developing, synclinal keel reoriented the stress patterns locally.

OTHER MEGAKINK BANDS IN THE N.S.W. SOUTH COAST REGION

Description

At least two other megakink bands occur in the N.S.W. south coast region (Fig. 2; see also Powell 1984, fig. 1). The Batemans Bay megakink band is dextral where it crosses the Budawang Synclinorium, but its geometry appears to change to sinistral further east in the Ordovician turbidites. Outcrop in the eastern half of Batemans Bay megakink band is sparse so that we are not as confident of its geometry there as in the region immediately east of the Budawang Synclinorium where domains E and F (Figs. 10a & b) define a large-scale chevron fold.

The Narooma megakink band (domain M, Fig. 11) is sinistral and has a zone of abundant minor kink folds and crenulation cleavage, the Mystery Bay kink zone, near its southern boundary (Fig. 2). Outcrop information is good along the coast (Wilson 1968), and in a 15 km wide E–W strip from the southern end of the Budawang Synclinorium to the coast (Cole 1982), but has not been obtained in the inland half of domain M (Fig. 11). At the southern kink-band boundary at Mystery Bay, the NNE-trending foliation of domain N (Fig. 11) swings more than 90° counter-clockwise in less than 500 m along the coast before returning to the regional NNW trend of domain M. The northern boundary of the Narooma megakink band runs approximately through the town of Narooma, but appears to be offset to the north where it crosses the Budawang Synclinorium (the kink boundary is between domains H and I, Fig. 11).

The Tuross megakink (Fig. 2) marks a change in orientation of F_1 structural elements, but is not well constrained by present map data. Further south, a megakink boundary may exist just south of Eden (Fig. 2), and at least one second-order kink zone cuts through the coastal outcrops south of Mallacoota (Wilson *et al.* 1982, area 7b).

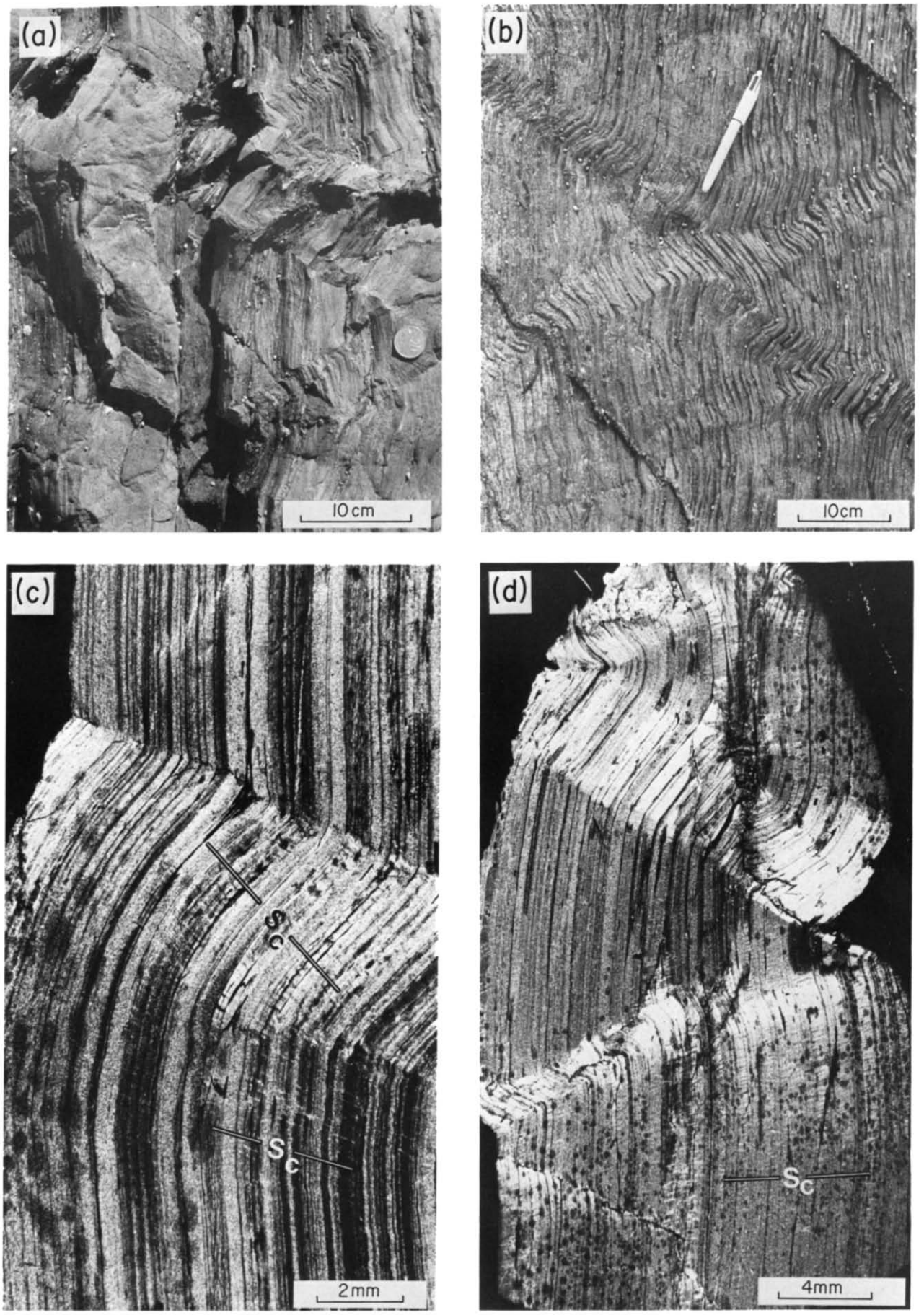

Fig. 7. (a) Outcrop-scale conjugate kinks from which layer-parallel shortening has been inferred, and principal-stress orientations calculated. (b) Conjugate kink bands in foliated psammopelite. Pen points north. (c) Thin-section of a 'bend-glide' kink fold (cf. Dewey 1965, fig. 9). Foliation outside the kink at the upper, angular kink plane makes a smaller angle (65°) with the kink plane than does adjacent foliation inside the kink (73°)—implying a dilatation of 5.5% normal to the foliation inside the kink band. This dilatation may be accounted for by the development of crenulation-microfolds with axial surfaces, S_c, at *c.* 75° to the foliation. S_c maintains a constant angle to the foliation around the lower, rounded hinge, suggesting that S_c formed before bulk rotation of the kink band. This bend-glide structure may be analogous to the structure of the Budawang Synclinorium west of Batemans Bay. Crossed nicols. (d) Conjugate kink bands with pervasive crenulation-microfold axial surfaces, S_c, developed parallel to the sinistral kink plane. Crossed nicols. All specimens are from outcrops *c.* 0.5 km south of Mystery Bay (see Powell 1983a, fig. 57).

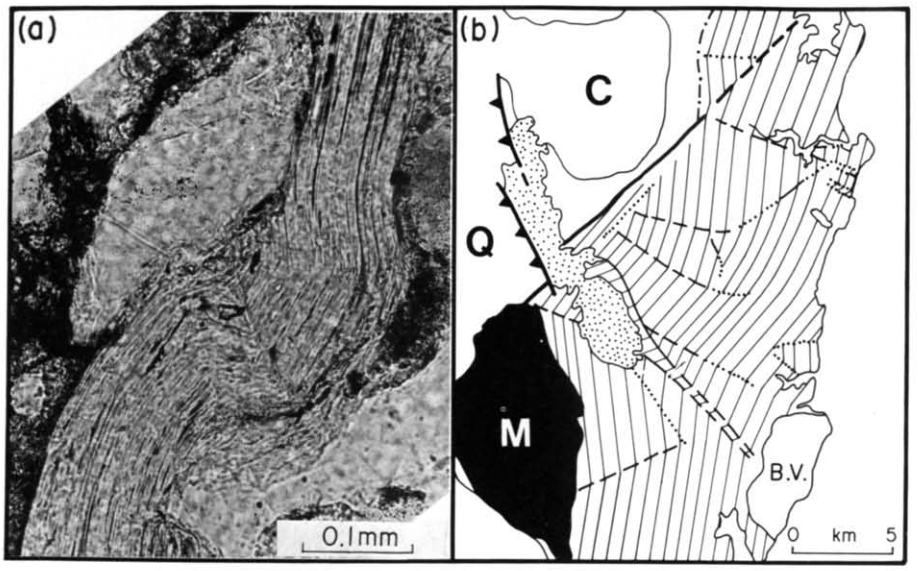

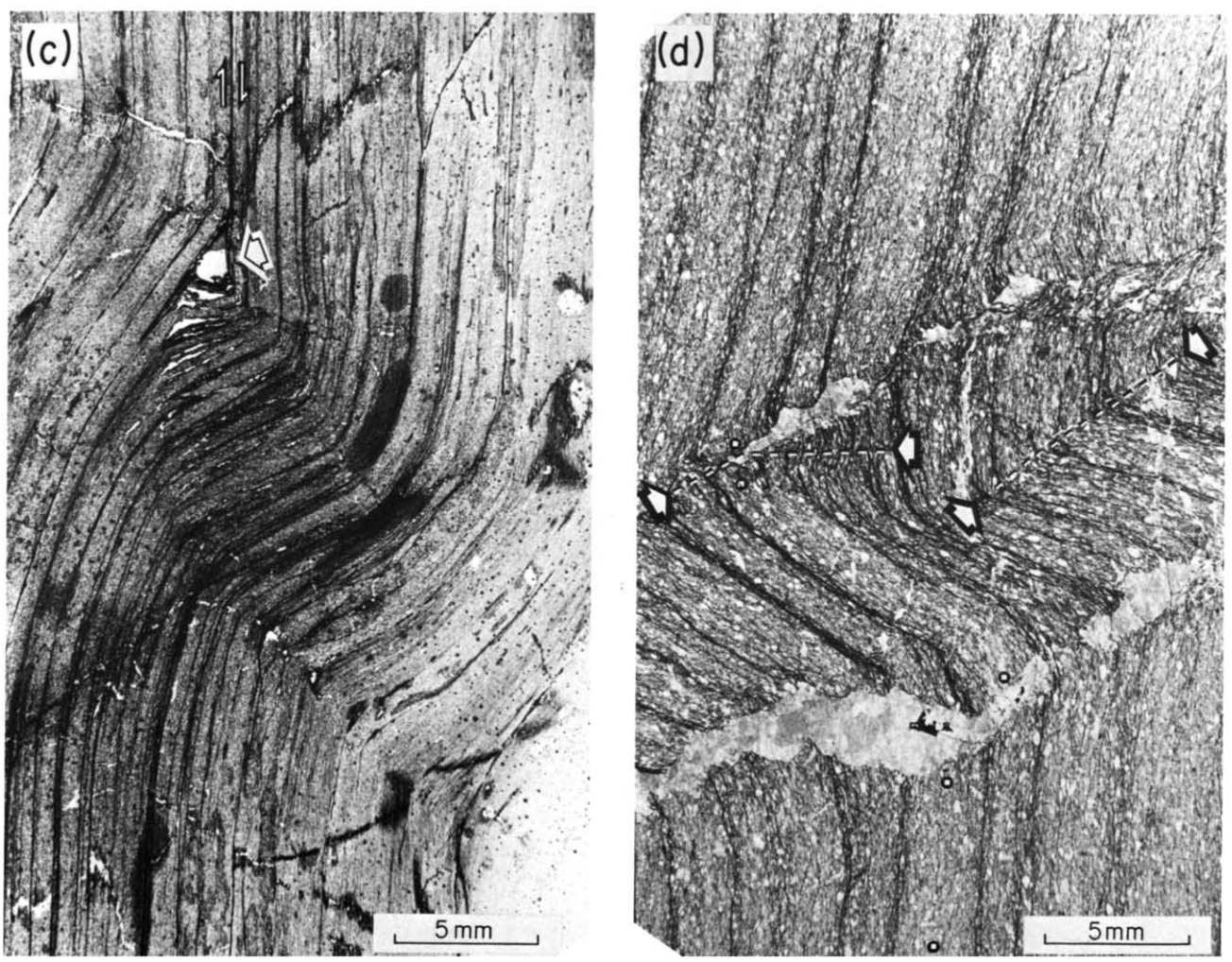

Fig. 8. Comparison of the geometry of (a) kinked detrital mica and (b) the Bermagui megakink band. (a) is from Conaghan & Powell (1982). C, Coolagoolite Granodiorite; Q, Quaama Granodiorite; M, Mumbulla Granite, all plutons of the Bega Batholith. Note the 7.5 orders of magnitude difference in scale. See text for further explanation. (c) Geometry of a dextral kink termination accommodated by dilatation (arrow) and layer-parallel slip (pair of half arrows, top centre). Note some bending of the external foliation adjacent to the kink planes, and the transition along the upper kink plane from a sharp, angular bend to a rounded fold (cf. Bermagui megakink band). Plane-polarized light. (d) A step in the position of the kink plane from one foliation surface to the next (see arrowed zones). The geometry may be analogous to the apparent northward step in the position of the Narooma megakink as it passes from the Ordovician coastal facies into the Budawang Synclinorium. Plane-polarized light. (c) and (d) are from the same outcrops near Mystery Bay referred to in Fig. 7.

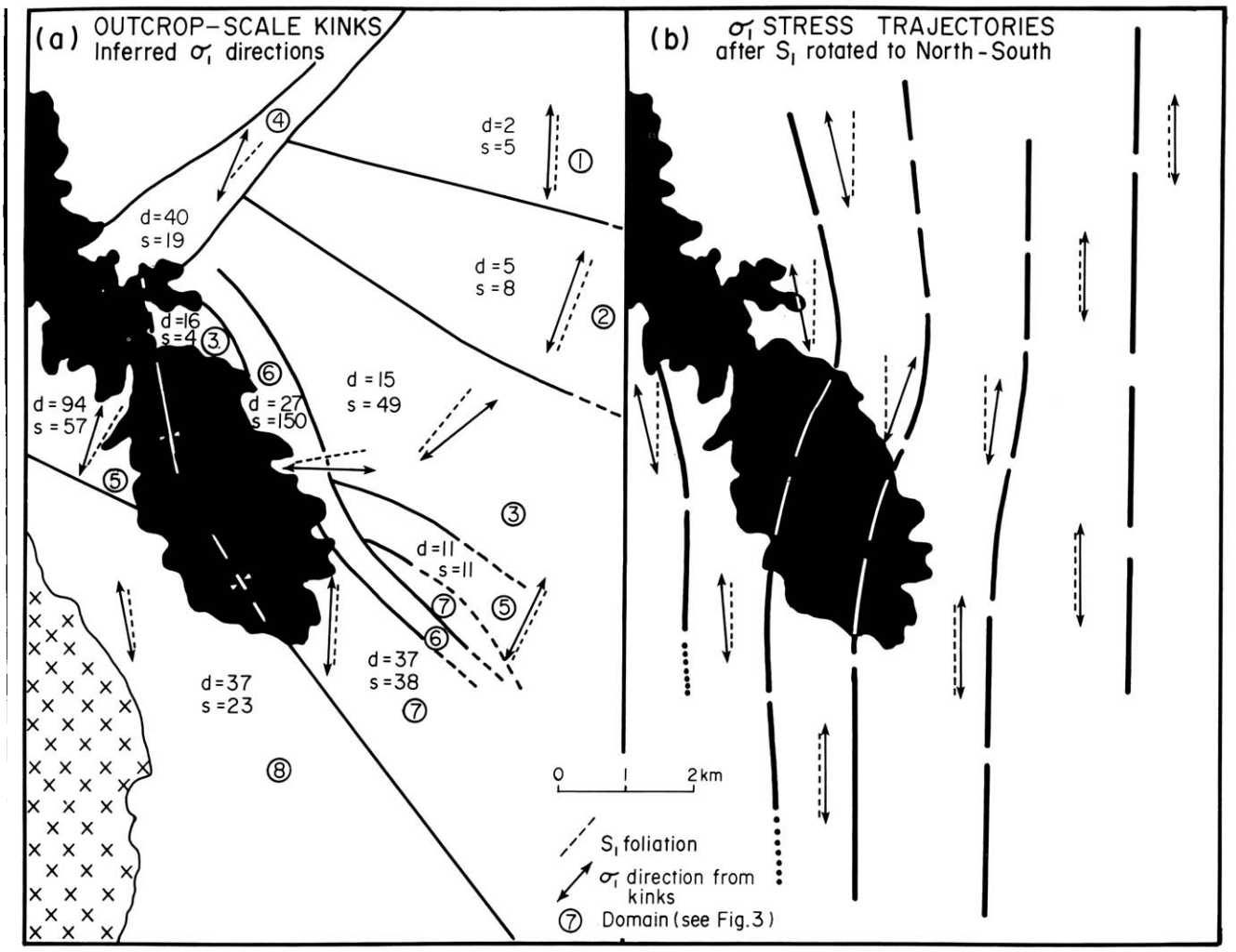

Fig. 9. Proportion of sinistral (s) to dextral (d) kinks in each of the Bermagui megakink domains, with σ_1 directions inferred using the kink-proportion method of Gay & Weiss (1974). (a) Present orientation. (b) With S_1 rotated to a common N–S orientation.

Kink rotation axes and interdomain angles

The structural elements summarized in stereogram form (Figs. 10 and 11) have been analysed statistically in the same way as those of the Bermagui megakink band. Summary stereograms for the mean π_1^0, L_1^0 and S_1 for each domain in the Batemans Bay and Narooma megakink bands (Fig. 12) show that the kink rotation axes are nearly vertical.

The angular changes across adjacent domains in the Batemans Bay and Narooma megakinks (Table 1) range from 17 to 57°, with 4 of the 8 angular changes being around 20°. The largest angular change is across the southeastern boundary of the Narooma megakink. These angular changes are less than those commonly measured in outcrop-scale kink bands (e.g. Anderson 1968) or produced experimentally in ideal foliated materials (e.g. Weiss 1968, Gay & Weiss 1974), but are similar to the small interdomain angles reported by Hobson (1973) from slates and schists near Tintagel, Cornwall. Dewey (1965, fig. 29) also noted kink bands with small interdomain angles in deformed kyanite, and McClay (1982, fig. 18c) noted similar structures in deformed pyrhhotite. Dewey (1965) suggested there was an intimate association between kink bands and bend-glide folds, and suggested that where kink bands are at a high angle to the foliation being kinked they may be the result of a polygonization process whereby elastic strain in the buckled foliation is being relieved. The megakinks in the easternmost Lachlan Fold Belt appear to be of this high-angle type, and consequently may have formed by processes analogous to those operating in deformed crystals and metals.

Table 1. Angular change across megakink domains

(a) Batemans Bay Megakink (Fig. 10)	
Domain pair	Angular change
A∧B	19°
B∧C	40°
D∧E	27°
E∧F	37°
F∧G	17°
E∧G	20°
(b) Narooma Megakink (Fig. 11)	
Domain pair	Angular change
H∧I	22°
L∧M	34°
M∧N	57°

Note: Angular change is estimated by taking the most reliable of mean π_1^0, L_1^0 and S_1 for each domain. Angular changes in the Bermagui megakink are given in Fig. 6(d).

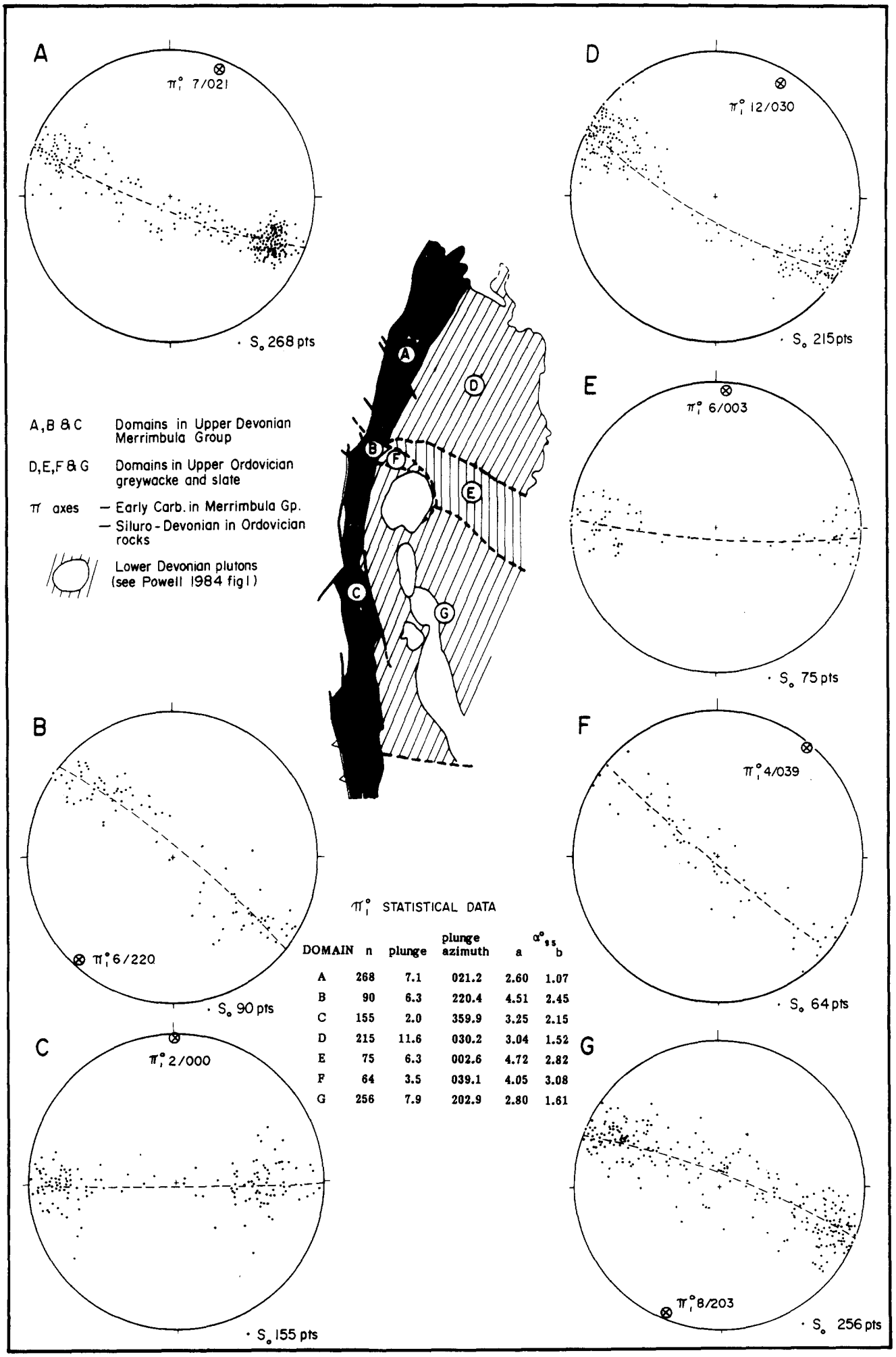

π_1° STATISTICAL DATA

DOMAIN	n	plunge	plunge azimuth	a	α°_{95} b
A	268	7.1	021.2	2.60	1.07
B	90	6.3	220.4	4.51	2.45
C	155	2.0	359.9	3.25	2.15
D	215	11.6	030.2	3.04	1.52
E	75	6.3	002.6	4.72	2.82
F	64	3.5	039.1	4.05	3.08
G	256	7.9	202.9	2.80	1.61

Fig. 10(a). Equal-area lower-hemisphere stereograms of bedding in F_1 structural elements in the Budawang Synclinorium (domains A, B and C) and the foliated Ordovician turbidites (domains D, E, F and G). Field data collected by Cole, Powell and students. Statistics computed by N. I. Fisher (see Appendix).

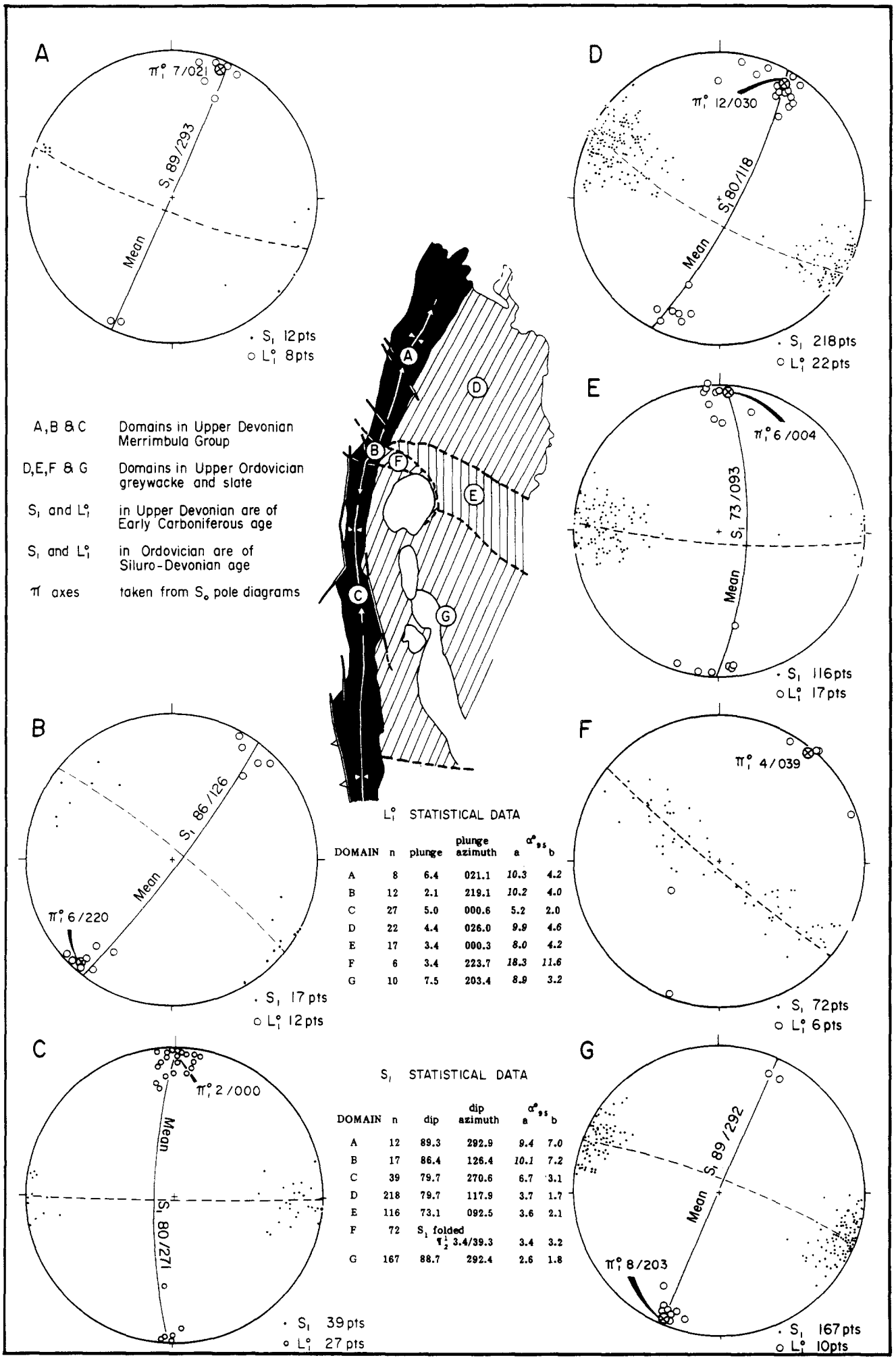

L°_{1} STATISTICAL DATA

DOMAIN	n	plunge	plunge azimuth	α°_{95} a	b
A	8	6.4	021.1	*10.3*	4.2
B	12	2.1	219.1	*10.2*	4.0
C	27	5.0	000.6	5.2	2.0
D	22	4.4	026.0	*9.9*	4.6
E	17	3.4	000.3	*8.0*	4.2
F	6	3.4	223.7	*18.3*	*11.6*
G	10	7.5	203.4	*8.9*	3.2

S_1 STATISTICAL DATA

DOMAIN	n	dip	dip azimuth	α°_{95} a	b
A	12	89.3	292.9	*9.4*	7.0
B	17	86.4	126.4	*10.1*	7.2
C	39	79.7	270.6	6.7	3.1
D	218	79.7	117.9	3.7	1.7
E	116	73.1	092.5	3.6	2.1
F	72	S_1 folded $\frac{1}{2}$	3.4/39.3	3.4	3.2
G	167	88.7	292.4	2.6	1.8

Fig. 10(b). Equal-area lower-hemisphere stereograms of S_1 cleavage and bedding/cleavage intersections (L^{0}_{1}) in the Budawang Synclinorium (domains A, B and C) and the foliated Ordovician turbidites (domains D, E, F and G). Field data sources and statistics as in Fig. 10(a).

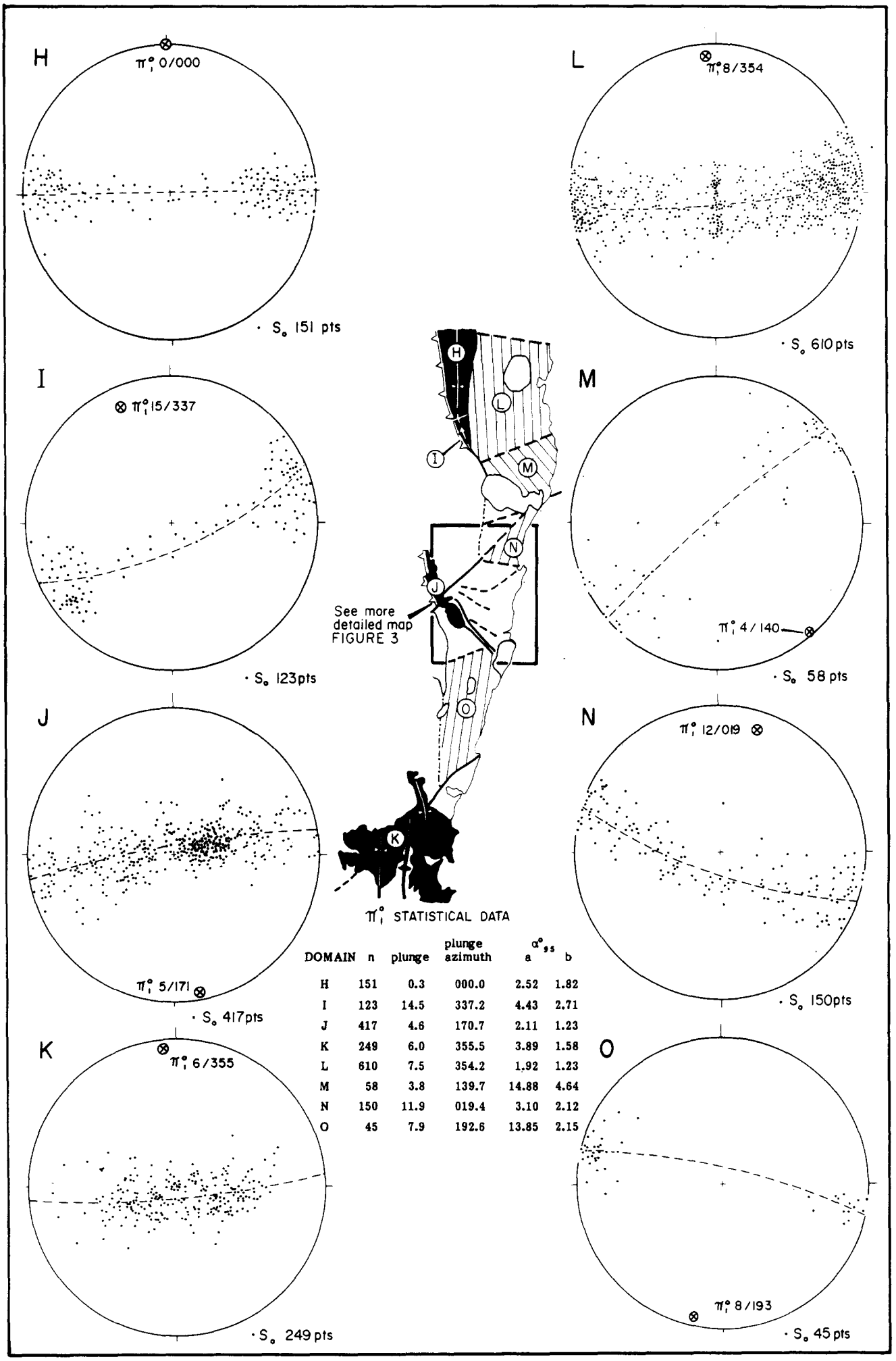

π°_1 STATISTICAL DATA

DOMAIN	n	plunge	plunge azimuth	α°_{95} a	b
H	151	0.3	000.0	2.52	1.82
I	123	14.5	337.2	4.43	2.71
J	417	4.6	170.7	2.11	1.23
K	249	6.0	355.5	3.89	1.58
L	610	7.5	354.2	1.92	1.23
M	58	3.8	139.7	14.88	4.64
N	150	11.9	019.4	3.10	2.12
O	45	7.9	192.6	13.85	2.15

Fig. 11(a). Equal-area lower-hemisphere stereograms of bedding in F_1 structural elements in the Merrimbula Group (domains H, I, J and K) and the foliated Ordovician turbidites (domains L, M, N and O). Field data sources: H: Cole & Fergusson (unpubl. data); I and L: Cole (1982); M: Wilson (1968); J, N and O: Cole, Conaghan, Powell & students; K: Fergusson (unpubl. data). Statistics computed by N. I. Fisher (see Appendix).

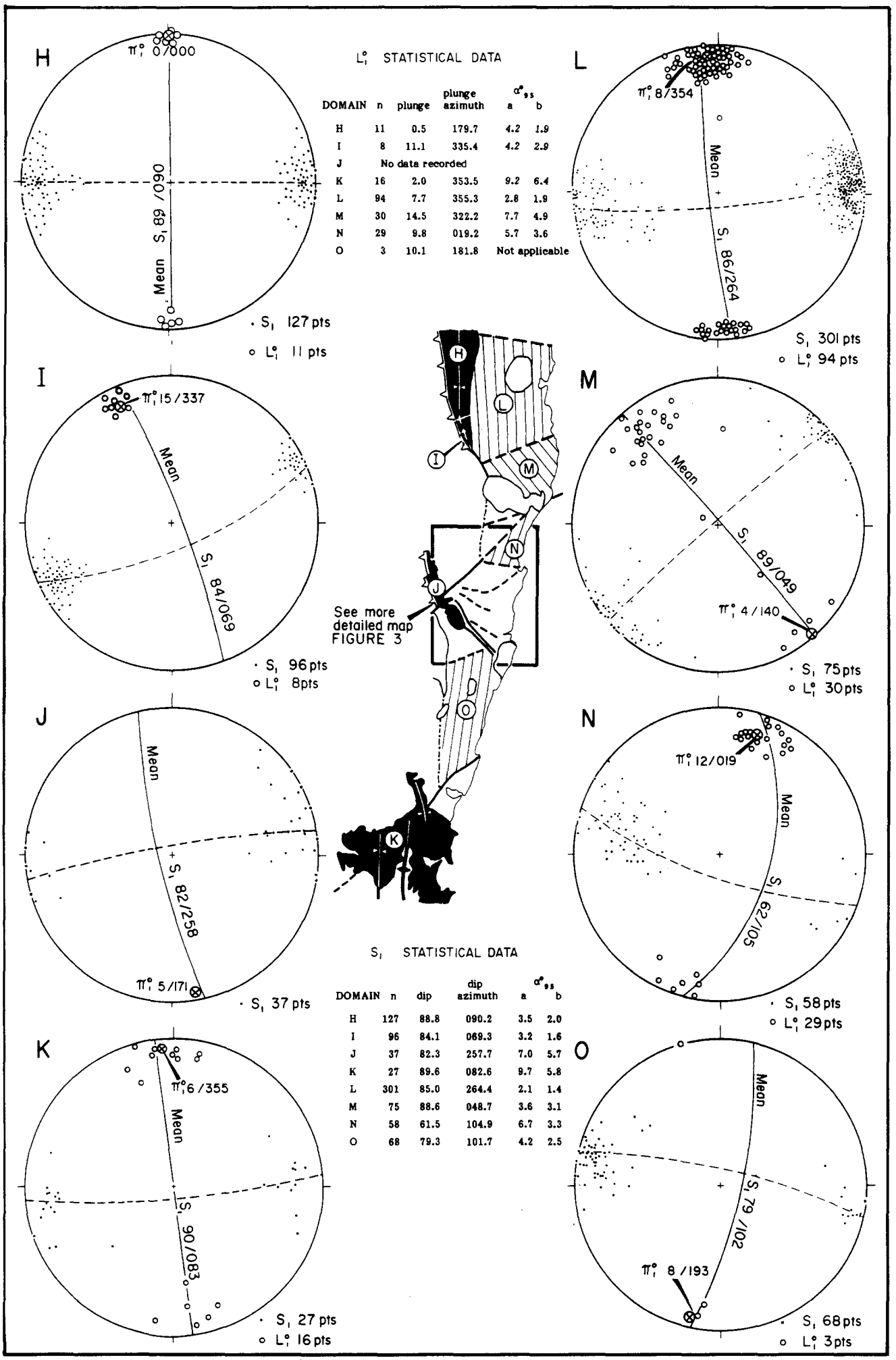

Fig. 11(b). Equal-area lower-hemisphere stereograms of S_1 cleavage and bedding/cleavage intersections (L_1^0) in the Merrimbula Group (domains H, I, J and K) and the foliated Ordovician turbidites (domains L, M, N and O). Field data sources and statistics as in Fig. 11(a).

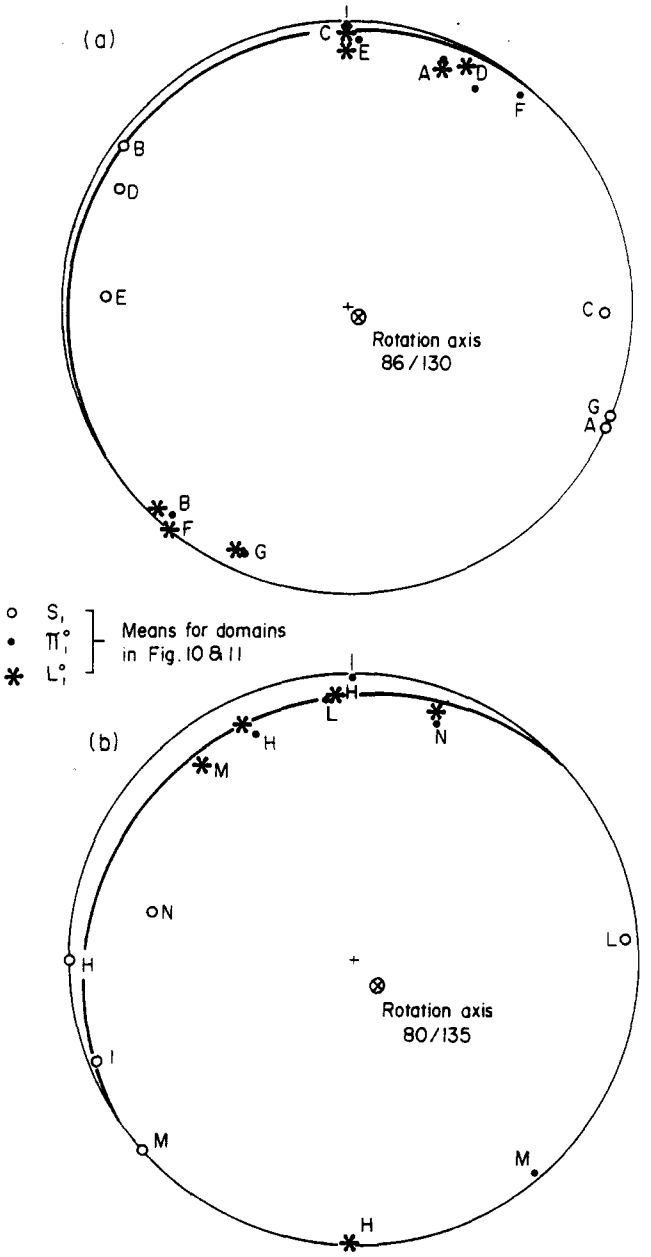

Fig. 12. Equal-area lower-hemisphere stereograms of mean S_1, L_1^0 and π_1^0 data from (a) Batemans Bay and (b) Narooma megakink bands. Best-fit π-circles calculated by inspection, taking into account the variable confidence cones for each domain. The apparently large discrepancy from the π-circle of S_1 in domain N is caused by refolding of S_1 by F_2 in a narrow zone running N–S through Bermagui.

INTERPRETATION

Relative timing of the megakinks, and the lower-order kink bands

In the Bermagui megakink band, the constant angular relationship between outcrop-scale kink bands and local S_1 in all domains, including those with high rotation, suggests that the outcrop-scale structures formed before any substantial rotation of the megakink domains. The only other place on the N.S.W. south coast where kink bands have been analysed to determine the orientation of the maximum principal compression is at Mystery Bay (Powell 1983a) where σ_1 is within 15° of the NNW-trending S_1 foliation. Other outcrop-scale structures include buckle folds and crenulation cleavages, the most common being a crenulation cleavage approximately parallel to the dextral kink plane. Mapping in the Bermagui megakink band (Cudahy 1983) and on the coast just south of Bermagui (Powell in prep.) has shown that these structures tend to maintain a constant orientation relative to the local S_1 foliation, and are thus rotated around the megakink and second-order kink bands. Accordingly, we conclude that the first increments of strain during the megakinking deformation were responsible for most of the outcrop-scale structures.

The relative timing of the megakinking and second-order kinking is more difficult to determine. In the Bermagui megakink band, the Murrah kink zone (domain 6) appears to cut across three of the megakink band domains (3, 5 and 7, Fig. 3). The second-order structure is a zone of higher-than-normal outcrop-scale kink-band strain, and is spatially related to the adjacent Merrimbula Group syncline. The Murrah kink zone is likely to be a concentration of strain that could not otherwise be accommodated by the (relatively) mechanically rigid synclinal keel. Other second-order kink zones, such as at the southern edge of Beares Beach and also near Jerimbut Point (Fig. 3), have no obvious relationship to structure in the Merrimbula Group, or to the megakink domains. Conceivably, megakinking and second-order kinking proceeded together, although we leave this question open.

Amount of shortening

The minimum amount of shortening involved in the megakinking can be determined by measuring the distance along a foliation trace and comparing it with the length of an assumed initially straight foliation trace. This method gives a minimum estimate of the amount of shortening because: (1) the interpreted map-linear foliation trace in any domain is the minimum possible length of the foliation in that domain and (2) the map-linear foliation trace does not take into account any shortening represented by outcrop-scale kink bands or second-order kink bands not recognized because of insufficient outcrop.

Applying the method to the Bermagui megakink band (Fig. 3), we estimate 1.2 ± 0.1 km of shortening over approximately 17 km in an 015° direction between domains N and O (Fig. 11). This corresponds to about 7% of NNE–SSW shortening. How much shortening should be added for the outcrop-scale kinking and possible unrecognized second-order kinking is a debatable point. Cudahy (1983) has estimated outcrop-scale shortening of as much as 16% in single outcrops, but in most outcrops where kink bands are present, the shortening is less than a third of this, and in outcrops where one or no kink band is present, the shortening may be negligible. Cudahy (1983) noted that the density of kinks is much higher within 1 or 2 km of the Merrimbula Group outcrop, and in this zone additional shortening due to outcrop-scale kinking may average 2 to 5%. However,

outside this radius, kink bands are rare and shortening attributable to outcrop-scale kink bands is probably less than 1%. We are thus fairly confident in estimating that the shortening parallel to foliation across the Bermagui megakink band is between 7 and 10%.

Applying the same method to the 160 km map strip between the southern edge of the Sydney Basin and the Burragate Fault near Tathra (Fig. 2), Powell (1984, fig. 2) estimated that the minimum shortening in an 015–195° direction was 4.5%. This estimate did not include any shortening attributable to outcrop-scale kink bands, and second-order kinks as yet unrecognized. However, Powell (1984) pointed out that outcrop-scale kink bands are common only in the second-order kink bands, and since these occupy less than 10% of the 160 km map area, their contribution to the overall shortening is likely to be less than 1%. Powell (1984) rounded the estimate of N–S shortening to 5%.

Timing of megakinking

The timing of megakinking is fairly well constrained by geological relationships near the southern margin of the Sydney Basin (Fig. 2). Two lines of argument indicate that the megakinking was a single event postdating the regional N–S folding in the Early Carboniferous around 350–340 Ma ago (Powell *et al.* 1977, Shaw *et al.* 1982). First, the Batemans Bay megakink band has deformed the Budawang Synclinorium which is one of the Early Carboniferous structures. Secondly, in the Ordovician turbidites the megakinking is the youngest folding event recognized, and deforms all the early structures including upright F_2 folds that are correlatable with the Early Carboniferous N–S folds in the Upper Devonian rocks (Powell 1983a).

The upper age limit is given by the relationship of the megakinked Lachlan Fold Belt to the Sydney Basin—a flat-lying sheet of cover sediment which lies with high-angle unconformity on the Devonian to Ordovician basement. Although no megakink zones have been mapped into the unconformity, we are fairly sure, from the gentle nature of structures in the Sydney Basin (Shepherd & Huntington 1981), that no major N–S shortening, of the order of 5% indicated by the megakinks, has affected these rocks. The megakinking thus antedates the oldest sediments of the Sydney Basin, which are of latest Carboniferous age (*c.* 300 Ma) (Herbert 1972).

These geological relationships thus constrain the megakinking to intra-Carboniferous, and, as Powell (1984) pointed out, megakinking may have been synchronous with mid-Carboniferous thrusting (340 to 320 Ma) in Central Australia (Wells *et al.* 1970, Armstrong & Stewart 1975, Wells & Moss 1983), and megafolding in north Queensland (Bell 1980).

Relation of megakinks to Landsat lineaments in the Lachlan Fold Belt

Some of the megakinks recognized in the foliated eastern belt line-up with major ENE- and ESE-trending lineaments recognized from LANDSAT images in the main part of the Lachlan Fold Belt to the west (Scheibner 1973, 1974a,b) (cf. Figs. 1 and 2). The Wiarborough megakink corresponds to the southern edge of the 50 km-wide band of lineaments collectively known as the Lachlan River lineament (Scheibner 1974b, Scheibner & Stevens 1974). This ESE-trending lineament extends right across the Lachlan Fold Belt (Fig. 1), and there is evidence that it was active from the Ordovician to the Carboniferous (Scheibner & Stevens 1974, Glen 1985). One segment of it in the western Lachlan Fold Belt, the Crowl Creek lineament, was active in the latest Silurian, late Early Devonian and the Carboniferous (Scheibner 1973, Glen 1982, 1985, Glen *et al.* in press). The northern edge of the Lachlan River lineament is the zone of lineaments passing ESE through Orange, and within the Lachlan River lineament the structure in both the Ordovician turbidites and the Upper Devonian rocks trends NNE in contrast to the N–S trends north and south of the lineament zone. This geometry is consistent with the entire 50 km long NNE-trending strip being a large dextral megakink band, in which case there is an integrated dextral offset of the Lachlan Fold Belt by 25 km across the Lachlan River lineament. Interestingly, the anomalous NNE-trending folds in the Upper Devonian Hervey Group near Grenfell (Conolly 1965), just northwest of the western edge of Fig. 2, also lie in the Lachlan River lineament.

The Narooma megakink band (Fig. 2) represents a sinistral offset of the regional N–S tectonic grain by 15–20 km parallel to the ENE-trending megakink plane. The southeastern margin of this megakink band, the Mystery Bay kink zone, is aligned with the Tantawangalo Fault, along which 16 km of dextral offset occurred in the Middle Devonian (Sims 1982).

The implication of these relationships is that some of the megakinks may have been nucleated over, or alongstrike of pre-existing lineaments. The inhomogeneity provided by a basement lineament, together with the concentration of strain likely when these lineaments were reactivated during mid-Carboniferous N–S compression, may have served to localize the megakinks.

DISCUSSION

The recognition of megakinks in the Lachlan Fold Belt has many interesting consequences. First, as far as we are aware, this is the first time kink-like structures of such large dimensions have been documented from fold belts, although Harrington *et al.* (1973) suggested they might be present in the Lachlan Fold Belt and Scheibner (1979) recognized 'gigantic kinking' associated with NW-trending lineaments south of Cobar. Second, because the megakinks are fairly tightly constrained to be intra-Carboniferous, and yet their position appears controlled by older lineaments, we have an example of the infliction or propagation of older trends into new

materials (Scheibner 1974c). In fact, the ENE- and ESE-trending lineaments in the Lachlan Fold Belt are themselves probably reflections of old directions in the Precambrian western two-thirds of Australia propagated into the Phanerozoic Tasman Orogen episodically during its growth. The megakink trends themselves are important lineament directions in the younger Sydney Basin (Scheibner 1976, Shepherd & Huntington 1981) continuing the imposition of old into new.

Third, if the amount of N–S shortening estimated from the mapped coastal terrane (*c.* 5%) can be extrapolated to the rest of the Tasman Orogen, there is a possible total of 150 km of mid-Carboniferous N–S shortening in eastern Australia. This is at the right time, and of the right order, to be equated with the mid-Carboniferous N–S shortening in central Australia during the Alice Springs Orogeny (Fig. 1, discussed in Powell 1984).

Fourth, we have noted buckle folds and crenulation cleavage associated with the megakinks. The crenulation cleavages occur in two directions. One, having a consistent dextral asymmetry to the associated crenulation microfolds, commonly develops at about 35° counterclockwise from the pre-existing S_1 foliation. The other has no preferred asymmetry to the associated crenulation microfolds and develops at a high angle (>70°) to the S_1 foliation. If these cleavages have developed under the same N–S compression that produced the associated outcrop-scale kinks, then neither lies perpendicular to the inferred direction of greatest compression. The nature and geometry of these cleavages is (or will be) described elsewhere (Cudahy 1983, in prep., Powell 1983a, in prep.).

Fifth, the generation of the segmented Bermagui megakink band and fault-bend folds (Suppe 1983) may be similar processes. Fault-bend folds form where fault blocks ride over non-planar fault surfaces, with the angular, kink-like folds forming opposite bends in the fault surface. The Bermagui megakink is located opposite such an irregularity where the N–S-trending foliated stripy-cleavage terrane is offset by the NE-trending Tantawangalo Fault (Fig. 2). Indeed, the geometrical similarity between the profiles in Suppe's fig. 23 (1983) and the Bermagui megakink map (Fig. 3) is striking.

Finally, there is a close analogy between the foliated terrane around the Bermagui megakink band (Fig. 8a), and the deformed detrital mica (Fig. 8b) published by Conaghan & Powell (1982). Not only does the structure of the bent mica resemble the segmented geometry of the Bermagui megakink band, but the mechanical analogy of the mica flake enclosed in a matrix of rigid grains may resemble the mechanical contrast in the Bermagui region where the foliated Ordovician turbidites were being kinked adjacent to the 'undeformed' Bega Batholith. In the grain-scale specimen (Fig. 8a), up to 15% of shortening represented as kink strain in the mica is taken up by intergranular movement between rigid quartz and lithic grains. Perhaps we should look more closely at the 'undeformed' Bega Batholith to see whether the equivalents of the intergranular matrix are present as shear zones within, or between adjacent plutons.

Acknowledgements—The field data on which this paper is based have been accumulated over a decade by Powell, Macquarie University colleagues, research assistants and students working mainly under Powell's direction. Cole mapped the Bodalla area in 1982, and subsequently extended the megakink map on a reconnaissance level from Batemans Bay to Eden. Cudahy mapped the Bermagui megakink area inland from the coast in 1983. Fergusson gathered data in 1977–1978 on the Ettrema and Eden areas, and inland from Narooma. N. I. Fisher analysed our data statistically, and P. Fell and J. Cole checked the results independently. P. J. Conaghan, T. Engelder, P. R. James, E. Scheibner and M. J. Rickard provided constructive criticism of an early draft. We thank Macquarie University and Australian Research Grants Scheme for supporting the many man-years of field work necessary to carry out the work.

REFERENCES

Anderson, T. B. 1968. The geometry of a natural orthorhombic system of kink bands. In: *Kink Bands and Brittle Deformation* (edited by Baer, A. J. & Norris, D. K.). *Geol. Surv. Pap. Can.* **68-52**, 200–226.

Armstrong, R. L. & Stewart, A. J. 1975. Rubidium–strontium dates and extraneous argon in the Arltunga Nappe Complex, Northern Territory. *J. geol. Soc. Aust.* **22**, 103–115.

Bell, T. H. 1980. The deformation history of northeastern Queensland—a new framework. In: *The Geology and Geophysics of Northeastern Australia* (edited by Henderson, R. A. & Stephenson, P. J.). *Geol. Soc. Aust. Qld. Div.*, Brisbane, 307–313.

Clifford, P. 1968. Kink band development in the St Joseph area, northern Ontario. In: *Kink Bands and Brittle Deformation* (edited by Baer, A. J. & Norris, D. K.). *Geol. Surv. Pap. Can.* **68-52**, 229–241.

Cheeney, R. F. 1983. *Statistical Methods in Geology*. George Allen & Unwin, London.

Cole, J. P. 1982. The structure and stratigraphy of the Bodalla area, N.S.W. Unpublished B.Sc.(Hons) thesis, Macquarie University, North Ryde, Australia.

Collomb, P. & Donzeau, M. 1974. Relations entre kink-bands decametrique et fractures de socle dans l'Hercynien des Monts D'Ougarta (Sahara Occidental Algerie). *Tectonophysics* **24**, 213–242.

Conaghan, P. J. & Powell, C. McA. 1982. Deformed detrital mica (I) & (II). In: *Atlas of Deformational and Metamorphic Rock Fabrics* (edited by Borradaile, G. J., Bayly, M. B. & Powell, C. McA.). Springer, Heidelberg, 414–417.

Conolly, J. R. 1965. The stratigraphy of the Hervey Group in central New South Wales. *J. Proc. R. Soc. N.S.W.* **98**, 37–83.

Cudahy, T. J. 1983. The Bermagui megakink and associated structures. Unpublished B.Sc.(Hons) thesis, Macquarie University, North Ryde, Australia.

Dewey, J. F. 1965. Nature and origin of kink bands. *Tectonophysics* **1**, 459–494.

Dewey, J. F. 1966. Kink bands in lower Carboniferous slates of Rush, Co. Dublin. *Geol. Mag.* **103**, 138–142.

Fyson, W. K. 1966. Structures in the Lower Palaeozoic Meguma Group, Nova Scotia. *Bull. geol. Soc. Am.* **77**, 931–944.

Gay, N. C. & Weiss, L. E. 1974. The relationship between principal stress directions and the geometry of kinks in foliated rocks. *Tectonophysics* **21**, 287–300.

Geological Society of Australia. 1971. *Tectonic Map of Australia and New Guinea, Scale* 1:5,000,000. Sydney.

Glen, R. A. 1982. Nature of late-Early to Middle Devonian tectonism in the Buckambool area, Cobar, New South Wales. *J. geol. Soc. Aust.* **29**, 127–138.

Glen, R. A., Powell, C. McA. & Khaiami, R. K. in press. The Mulga Downs Group. In: *Geology of the Wrightville* 1:100,000 *sheet 8034* (edited by Glen, R. A.). *Geol. Surv. N.S.W. Explan. Notes*, Sydney.

Glen, R. A. 1985. Basement control on the deformation of cover basins: an example from the Cobar district in the Lachlan Fold Belt, Australia. *J. Struct. Geol.* **7**, 301–315.

Harrington, H. J., Burns, K. L. & Thompson, B. R. 1973. Gambier–Beaconsfield and Gambier–Sorell Fracture Zones and the movement of plates in the Australia–Antarctica–New Zealand region. *Nature, Lond.* **245**, 109–112.

Herbert, C. 1972. Palaeodrainage patterns in the southern Sydney Basin. *Rec. geol. Surv. N.S.W.* **14**, 5–18.
Hobson, D. M. 1973. The origin of kink bands near Tintagel, North Cornwall. *Geol. Mag.* **110**, 133–144.
Marshall, B. 1964. Kink bands and related geological structures. *Nature, Lond.* **204**, 772–773.
McClay, K. R. 1982. Fabrics in ores: pyrrhotite. In: *Atlas of Deformational and Metamorphic Rock Fabrics* (edited by Borradaile, G. J., Bayly, M. B. & Powell, C. McA.). Springer, Heidelberg, 74–75.
Powell, C. McA. 1983a. Geology of the N.S.W. South Coast and adjacent Victoria with emphasis on the Pre-Permian structural history. *Geol. Soc. Aust. SGTSG Field Guide* **1**, 1–118.
Powell, C. McA. 1983b. Tectonic relationship between the Late Ordovician and Late Silurian palaeogeographies of southeastern Australia. *J. geol. Soc. Aust.* **30**, 353–373.
Powell, C. McA. 1984. Terminal fold-belt deformation: relationship of mid-Carboniferous megakinks in the Tasman fold belt to coeval thrusts in cratonic Australia. *Geology* **12**, 546–549.
Powell, C. McA., Edgecombe, D. R., Henry, N. M. & Jones, J. G. 1977. Timing of regional deformation of the Hill End Trough: a reassessment. *J. geol. Soc. Aust.* **23**, 407–421.
Prentice, M. J. 1984. A distribution-free method of interval estimation for unsigned directional data. *Biometrika* **71**, 147–154.
Ramsay, J. G. 1962. The geometry of conjugate fold systems. *Geol. Mag.* **99**, 516–526.
Rixon, L. K., Bucknell, W. R. & Rickard, M. J. 1983. Megakink folds and related structures in the Upper Devonian Merrimbula Group, South Coast, N.S.W. *J. geol. Soc. Aust.* **30**, 277–293.
Scheibner, E. 1973. ERTS-1 geological investigations of New South Wales. *Geol. Surv. N.S.W.* Unpublished report GS 1973/382.
Scheibner, E. 1974a. *Tectonic Map of New South Wales, Scale* 1:1,000,000. *Geol. Surv. N.S.W.*, Sydney.
Scheibner, E. 1974b. Fossil fracture zones, segmentation and correlation problems in the Tasman Fold Belt system. In: *The Tasman Geosyncline—A symposium. Geol. Soc. Aust. Qld. Div.*, Brisbane, 65–98.
Scheibner, E. 1974c. Theory of lateral propagation (infliction, imposition) of major shears. *Utah. geol. Ass. Publ.* **5**, 604–608.
Scheibner, E. 1976. *Explanatory Notes on the Tectonic Map of New South Wales, Scale* 1:1 000 000. *Geol. Surv. N.S.W.*, Sydney.
Scheibner, E. 1979. Geological significance of some lineaments in New South Wales. *Proc. 1st Austral. Remote Sensing Conf., LANDSAT* 79, Sydney, 318–332.
Scheibner, E. & Stevens, B. P. J. 1974. The Lachlan River lineament and its relationship to metallic deposits. *Q. Notes geol. Surv. N.S.W.* **14**, 8–18.
Shaw, S. E., Flood, R. H. & Riley, G. H. 1982. The Wologorong Batholith, New South Wales, and the extension of the I–S line of the Siluro-Devonian granitoids. *J. geol. Soc. Aust.* **29**, 41–48.
Shepherd, J. & Huntington, J. F. 1981. Geological fracture mapping in coalfields and the stress fields of the Sydney Basin. *J. geol. Soc. Aust.* **28**, 299–309.
Sims, D. S. 1982. The Tantawangalo Fault. Unpublished B.Sc.(Hons) thesis, Macquarie University, North Ryde, Australia.
Suppe, J. 1983. Geometry and kinematics of fault-bend folding. *Am. J. Sci.* **283**, 684–721.
Watson, G. S. in press. The calculation of confidence regions for eigenvectors. *Aust. J. Statist.* **26**.
Weiss, L. E. 1968. Flexural-slip folding of foliated model materials. In: *Kink Bands and Brittle Deformation* (edited by Baer, A. J. & Norris, D. K.). *Geol. Surv. Pap. Can.* **68-52**, 294–359.
Wells, A. T. & Moss, F. J. 1983. The Ngalia Basin, Northern Territory: the stratigraphy and structure. *Bull. Bur. Miner. Resour. Aust.* **212**.
Wells, A. T., Forman, D. J., Ranford, L. C. & Cook, P. J. 1970. Geology of the Amadeus Basin, Central Australia. *Bull. Bur. Miner. Resour. Aust.* **100**.
Williams, P. F. 1971. Structural analysis of the Bermagui area, N.S.W. *J. geol. Soc. Aust.* **18**, 215–228.
Williams, P. F. 1972. Development of metamorphic layering and cleavage in low-grade metamorphic rocks at Bermagui, Australia. *Am. J. Sci.* **272**, 1–47.
Williams, P. F. 1982. Differentiated layering. In: *Atlas of Deformational and Metamorphic Rock Fabrics* (edited by Borradaile, G. J., Bayly, M. B. & Powell, C. McA.). Springer, Heidelberg, 526–527.
Wilson, C. J. L. 1968. Geology of the Narooma area, N.S.W. *J. Proc. R. Soc. N.S.W.* **101**, 147–157.
Wilson, C. J. L., Harris, L. B. & Richards, A. L. 1982. Structure of the Mallacoota area, Victoria. *J. geol. Soc. Aust.* **29**, 91–105.

APPENDIX

N. I. Fisher

Calculation of an approximate elliptical confidence cone for the polar axis of a bipolar or girdle distribution, based on a large sample of measurements

Introduction

Two types of distributions for axial data which arise commonly in structural geology are bipolar distributions and girdle, or great-circle, distributions. Examples of bipolar data are given in Figs. 4, 10(b) and 11(b) in this paper, and of girdle data in Figs. 10(a) and 11(a). Bipolar data can be usefully summarized by calculating the principal axis of the data, and girdle data summarized by the polar axis to the best-fitting great circle. For large samples of measurements (e.g. at least 30), an approximate elliptical confidence cone can be associated with either of these summary axes. The method of obtaining such a confidence region is described below. First, some terminology is established to link geological notation with statistical notation.

Preliminary calculations

Suppose that the data set comprises measurements $(D_1, A_1), \ldots, (D_n, A_n)$ of plunge and plunge azimuth of n axes, or n poles to planes. The data are transformed to direction cosines $(x_1, y_1, z_1), \ldots, (x_n, y_n, z_n)$, where $x_i = \cos D_i \cos A_i$, $y_i = -\cos D_i \sin A_i$, $z_i = -\sin D_i$, $i = 1, \ldots, n$. (Note: D_i and A_i have to be converted to radian measure). The orientation matrix is then defined by

$$\mathbf{T} = \frac{1}{n}\begin{pmatrix} \sum x_i^2 & \sum x_i y_i & \sum x_i z_i \\ \sum x_i y_i & \sum y_i^2 & \sum y_i z_i \\ \sum x_i z_i & \sum y_i z_i & \sum z_i^2 \end{pmatrix}$$

An eigen-analysis is performed on $\mathbf{T}$, to obtain the eigenvalues $\Upsilon_1, \Upsilon_2, \Upsilon_3$, and corresponding eigenvectors $\boldsymbol{v}_1, \boldsymbol{v}_2, \boldsymbol{v}_3$. (Programs to calculate eigenvalues and eigenvectors of symmetric matrices are available on most computers.) Note that $\Upsilon_1 \geqq 0, \Upsilon_2 \geqq 0, \Upsilon_3 \geqq 0$ and $\Upsilon_1 + \Upsilon_2 + \Upsilon_3 = 1$. We assume that $\Upsilon_1 \leqq \Upsilon_2 \leqq \Upsilon_3$.

For bipolar data, Υ_3 will be large relative to Υ_2 and Υ_1; the corresponding eigenvector $\boldsymbol{v}_3$ is the principal axis of the data. For girdle data, Υ_3 and Υ_2 will each be large relative to Υ_1; the eigenvector $\boldsymbol{v}_1$ is then the polar axis to the best-fitting great circle. We shall denote the direction cosines of $\boldsymbol{v}_i$ by $(\lambda_i, \mu_i, \nu_i)$, $i = 1, 2, 3$.

Calculation of major and minor semi-axes of elliptical confidence cone

In this section I describe how to calculate the magnitudes of the major and minor semi-axes of an approximate confidence ellipse for the principal or polar axis. The procedure for determining the directions of the major and minor semi-axes is rather more involved, and outside the scope of this appendix.

(a) *Bipolar data.* Define:

$$e_{11} = [n(\Upsilon_2 - \Upsilon_3)^2]^{-1} \sum_{i=1}^{n} b_i^2 c_i^2$$

$$e_{22} = [n(\Upsilon_1 - \Upsilon_3)^2]^{-1} \sum_{i=1}^{n} a_i^2 c_i^2$$

$$e_{12} = e_{21} = [n(\Upsilon_1 - \Upsilon_3)(\Upsilon_2 - \Upsilon_3)]^{-1} \sum_{i=1}^{n} a_i b_i c_i^2,$$

where, for each i, $i = 1, \ldots, n$,

$$a_i = \lambda_1 x_i + \mu_1 y_i + \nu_1 z_i$$
$$b_i = \lambda_2 x_i + \mu_2 y_i + \nu_2 z_i$$

and

$$c_i = \lambda_3 x_i + \mu_3 y_i + \nu_3 z_i,$$

and set up the symmetric matrix

$$\mathbf{E} = \begin{pmatrix} e_{11} & e_{12} \\ e_{21} & e_{22} \end{pmatrix}.$$

Compute the inverse matrix $\mathbf{F} = \mathbf{E}^{-1}$ with elements

$$\mathbf{F} = \begin{pmatrix} f_{11} & f_{12} \\ f_{21} & f_{22} \end{pmatrix} \quad (f_{12} = f_{21})$$

and calculate the eigenvalues of $\mathbf{F}$, δ_1 and δ_2 say, where $0 < \delta_1 < \delta_2$. Suppose we are interested in a $100(1 - \alpha)\%$ confidence cone. The major and minor semi-axes are, respectively, arc sin $\{[-2 \log (\alpha)/(n\delta_1)]^{1/2}\}$ and arc sin $\{[-2 \log (\alpha)/(n\delta_2)]^{1/2}\}$ where log denotes natural logarithm, and these semi-axes have to be converted back to degrees.

(b) *Girdle data.* Carry out the procedure for bipolar data, except with the elements of $\mathbf{E}$ defined by

$$e_{11} = [n(Y_1 - Y_2)^2]^{-1} \sum_{i=1}^{n} a_i^2 b_i^2$$

$$e_{22} = [n(Y_1 - Y_3)^2]^{-1} \sum_{i=1}^{n} a_i^2 c_i^2$$

$$e_{12} = e_{21} = [n(Y_1 - Y_2)(Y_1 - Y_3)]^{-1} \sum_{i=1}^{n} a_i^2 b_i c_i.$$

The theory behind these large-sample confidence regions is given by Prentice (1984) and Watson (1984).